Curie transition of superparamagnetic nickel nanoparticles in silica glass: A phase transition in a finite size system

H. Amekura,* Y. Fudamoto, Y. Takeda, and N. Kishimoto
Nanomaterials Laboratory, National Institute for Materials Science, 3-13 Sakura, Tsukuba, Ibaraki 305-0003, Japan
(Received 22 October 2004; published 23 May 2005)

Magnetization of Ni nanoparticles (mean diameter of ~3 nm) in silica glass (SiO_2) has been studied up to ~375 °C, in comparison with that of Ni film (thickness of ~120 nm). At room temperature, the nanoparticles (NPs) show a Langevin loop without hysteresis which is characteristic in superparamagnetic NPs. The saturation magnetization of the NPs decreases more steeply than the bulk with increasing temperature. However, a certain amount of magnetization remains in the NPs, even above the bulk Curie temperature. Quantum Monte-Carlo simulation was carried out using an Ising spin model on the fcc lattice of $L\times L\times L$ ($L=3$ to 38). The experimental results are qualitatively reproduced with the model; i.e., the steep decrease of the saturation magnetization with increasing temperature and the residual magnetization above the bulk Curie temperature are both ascribed to the finite size effects.

DOI: 10.1103/PhysRevB.71.172404 PACS number(s): 75.75.+a, 02.70.Ss, 36.40.Ei, 75.20.−g

Phase transition is one of the central concepts of the condensed matter physics. According to a classical definition, phase transition is only defined in an infinite system ($N\rightarrow\infty$), where N denotes the number of constitutional units of the system. However, some finite size systems, e.g., clusters and nanoparticles, show nonmetal-metal, nonmagnetic-magnetic, solid-liquid transitions, and so on.[1,2] Superparamagnetism[3–5] has been observed in monodomain nanoparticles (NPs) whose constitutional atoms ferromagnetically interact with neighboring atoms. When the number of the constitutional atoms is small enough, all the constitutional spins simultaneously flip by thermal fluctuation. Each NP then behaves as a paramagnetic spin with a giant magnetic moment $\mu=-gJ\mu_B$, where g, μ_B, and J denote, respectively, the g factor, the Bohr magneton, and the angular momentum quantum number, which is on the order of the number of the constitutional atoms of the NP.[3–5] Although often a superparamagnetic NP is described as a giant spin and this description is practically useful, the description is not adequate at high temperature, where each spin of the constitutional atoms is largely fluctuated. Nikolaev *et al.*[6] described temperature dependence and the Curie transition of an ensemble of superparamagnetic NPs, using phenomenological equations. However, their theory did not consider that each NP consists of the finite number of atoms. This work is devoted to an experimental study of the Curie transition of the superparamagnetic Ni NPs. The results are not explained by Nikolaev's theory. Quantum Monte-Carlo simulations of the Curie transition of NP are carried out to explain the observed behaviors.

Two types of samples, Ni thin films on SiO_2 substrates and Ni NPs in SiO_2, were used. Optical grade silica glasses (KU-1: OH^- 820 ppm) of 15 mm in diameter and 0.5 mm in thickness were used for substrates of the both types. The Ni films were vacuum deposited on the SiO_2 substrates by resistive heating under a base pressure of less than $\sim1\times10^{-4}$ Pa. The film thickness of ~120 nm was determined by a step-height profiler.

The Ni NPs were fabricated by implantation of Ni negative-ions of 60 keV to SiO_2, using a Cs-assisted plasma-sputter type negative-ion source.[7] The ion flux and the fluence were 56 $\mu A/cm^2$ and 3.8×10^{16} ions/cm^2, respectively. According to Monte-Carlo ion-range simulation code SRIM2000,[8] the projectile range of Ni ions of 60 keV and the averaged atomic fraction of Ni over the ion range are 47 nm and ~0.10, respectively, in SiO_2. Transmission electron microscopy (TEM) showed that Ni NPs of 2.9 nm in mean diameter spontaneously formed within a surface layer of ~100 nm thick without heat treatments.[9]

Magnetization was evaluated by magneto-optical Kerr effects (Kerr rotation θ_K and Kerr ellipticity η_K) detected by the optical retardation modulation method. Details of the Kerr measurements were reported in Ref. 10. Magnetic field was applied normal to the sample surface up to ~21 kOe. The monochromatic light ($\lambda=200-900$ nm, $\Delta\lambda\sim1$ nm) from a 150 W Xe lamp through a 30 cm single monochromator was used. Although the ellipticity signal from SiO_2 substrate was negligible, the rotation signal from the substrate was too strong to be neglected. Hereafter, the rotation signal is shown after subtracting the linear component due to the SiO_2 substrate.

Temperature dependence measurements were carried out at 27–375 °C under monochromatic light illumination at fixed wavelengths. A sample was mounted on a temperature-controlled copper block in the box with a hole for light illumination and detection. Although there is no window material on the hole, the sample was separated from air by N_2 gas flow in the box. To exclude annealing effects under measurements, the samples were annealed at 400 °C for 1 h in N_2 gas flow before the measurements.

Figure 1 shows Kerr ellipticity ($\propto$ magnetization) loops of the Ni film at different temperatures, monitored at the wavelength of 330 nm. At room temperature, the Kerr ellipticity loop shows typical parallelogrammic loops with hysteresis, which are characteristic in ferromagnetic materials. (The hysteresis is difficult to be distinguished in Fig. 1, because of low magnification.) The coercive field is ~0.178 kOe at 27 °C, and gradually decreases with increasing temperature.

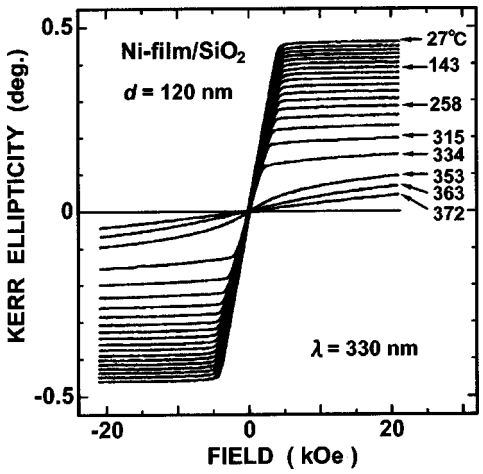

FIG. 1. Magnetization loops of 120-nm-thick Ni-film on silica glass detected by Kerr ellipticity at the wavelength of 330 nm at various temperatures between 27 and 372 °C.

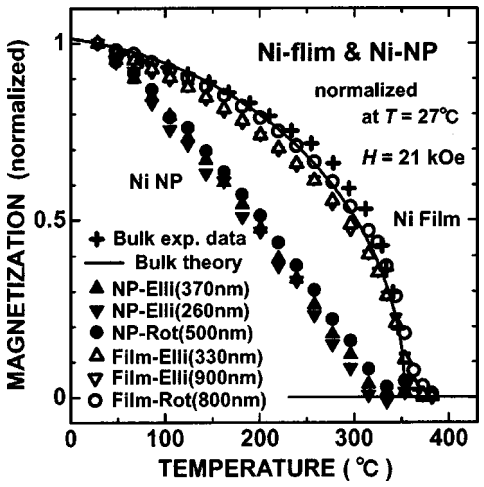

FIG. 2. Temperature dependences of magnetization normalized at 27 °C of Ni film on silica glass (open symbols) and Ni nanoparticles in silica glass (closed symbols). Closed upward triangles, downward triangles, and circles indicate magnetization of Ni nanoparticles determined by Kerr ellipticity at 370 and 260 nm and by Kerr rotation at 500 nm, respectively. Open upward triangles, downward triangles and circles indicate magnetization of Ni film determined by Kerr ellipticity at 330 and 900 nm, and by Kerr rotation at 800 nm, respectively. Crosses indicate literature data (see Ref. 11) of bulk Ni determined by static magnetization measurements. The solid line indicates a theoretical value of three-dimensional Ising model of $S=1/2$, solved by the mean-field approximation (see Ref. 11).

A field of ~4 kOe was required for the magnetization saturation, which is much higher than the value of bulk Ni [less than 0.2 kOe (see Ref. 11)]. However, the high saturation field is due to the large demagnetization field from the polar Kerr configuration where the field is applied normal to the film surface. With increasing temperature up to 334 °C, the saturation magnetization (ellipticity) decreases, but the parallelogrammic shapes are unchanged. At 353 °C, the loop suddenly changes to a paramagnetic-like curve without hysteresis. Above 363 °C, the loops are well fitted with straight lines. Since the bulk Curie temperature of Ni is reported[11] as 354 °C, the sudden change observed around 353 °C is ascribed to the Curie transition of the Ni film. The magnetizations at the maximum applied field (21 kOe) which correspond to the saturation magnetization up to 334 °C are plotted against temperature in Fig. 2. The saturation magnetizations evaluated at different wavelengths and different Kerr modes, i.e., the ellipticity modes at 330 and 900 nm, and the rotation mode at 800 nm, are all plotted in Fig. 2. All the data show similar dependence. The measured dependences were compared with literature data[11] of saturation magnetization of bulk Ni determined by static magnetization measurements. The dependences coincide with each other within experimental errors. This indicates that the Ni film of ~120 nm in thickness is enough thick to have the bulk nature.

In the case of Ni NPs in SiO_2, both the Kerr rotation and ellipticity loops follow a typical Langevin function[5] without hysteresis, which is characteristic in superparamagnetic NPs. The Langevin function[5] is described as

$$M(H,T) = M_S(T)L\left(\frac{\mu(T)H}{kT}\right), \quad \text{where } L(x) = \coth(x) - \frac{1}{x} \tag{1}$$

and M_s, μ, and k denote the saturation magnetization of the NPs system, the averaged magnetic moment per NP, and the Boltzman constant, respectively. Figure 3 shows Kerr ellipticity loops of the Ni NPs at different temperatures, monitored at a wavelength of 370 nm. The observed loops in the entire temperature range (27–375 °C) were well fitted with Eq. (1), and the saturation magnetization $M_s(T)$ and the averaged magnetic moment per NP $\mu(T)$ have been determined at given temperatures. At RT, the averaged magnetic moment per NP μ was as large as $4.0\times10^3\mu_B$ per NP, where μ_B is the Bohr magneton. One of the simplest explanations is that the magnetic NPs include $\sim4\times10^3$ Ni atoms in average, since $\mu=-g\mu_B NS \sim -N\mu_B$, where g, S, and N denote the g

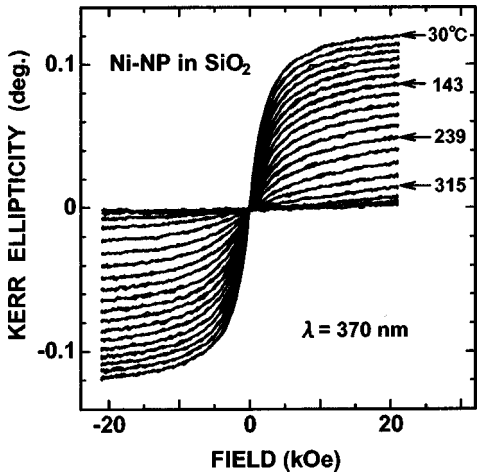

FIG. 3. Magnetization loops of Ni nanoparticles in silica glass detected by Kerr ellipticity at the wavelength of 370 nm at various temperatures between 27 and 351 °C.

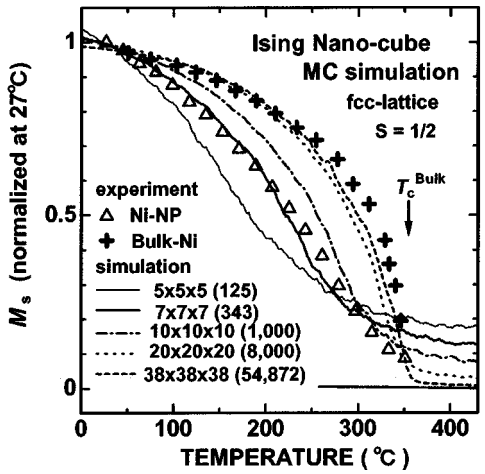

FIG. 4. Temperature dependence of saturation magnetization obtained by the quantum Monte-Carlo simulations of $S=1/2$ Ising cube ($L\times L\times L$ fcc lattice). Thin solid line, thick solid line, dotted chain line, dotted line, and broken line denote simulation results of $L=5$, 7, 10, 20, and 38 (i.e., total spin number per cube $N=L^3=125$, 343, 1000, 8000, and 54 872), respectively. Experimental results of saturation magnetization (extrapolated to $H\rightarrow\infty$) of Ni nanoparticles and bulk Ni are indicated by triangles and crosses, respectively.

factor ~ 2, spin quantum number $S\sim 1/2$ for Ni, and the number of Ni atoms per NP, respectively. However, the value $\sim 4\times 10^3$ is an averaged number of Ni atoms included per *magnetic* NP. The magnetization of Ni metal is due to itinerant 3*d* electrons. Very small NPs are no longer metals, because of the discreteness of the energy levels. Thus, very small (nonmetallic) Ni NPs show different magnetic moments from those due to itinerant 3*d* electrons. Probably smaller NPs than a critical size show much weaker magnetization than the itinerant ferromagnetism.[12] The Langevin fitting gives a mean value of $\sim 4\times 10^3$ atoms/NP, which were averaged over magnetic NPs only.

On the other hand, a value of 1.6×10^3 Ni atoms/NP on average is obtained from a mean diameter of Ni NPs of 2.9 nm determined by TEM observation,[9] with using the bulk Ni density. However, this is the mean value averaged over both NPs, magnetic and nonmagnetic. This value is smaller than that obtained by a magnetic measurements, since smaller NPs than the critical size are nonmagnetic[12] and do not contribute to magnetic measurements.

With increasing the temperature, the saturation magnetization $M_s(T)$ decreases. However, no clear transition was observed in the loop shape. Temperature dependence of M_s of Ni NPs is plotted in Fig. 4 and compared with the dependence of bulk Ni. The M_s of NPs decreases more steeply than the M_s of bulk Ni. However, even at the bulk Curie temperature, a small but certain value of M_s was observed in NPs. These behaviors cannot be expected by the Nikolaev's theory.[6]

To understand these temperature dependences which are different from the bulk Ni, a Ni NP was modeled as a *cube* instead of a *particle*. Since the bulk Ni shows a temperature dependence of M_s which is well fitted with $S=1/2$ Ising model,[11] and since the bulk Ni has fcc structure, the nanocube consists of the $S=1/2$ Ising spins, forming an fcc lattice of finite size ($L\times L\times L$, $L=3\sim 38$; i.e., $N=L^3=27\sim 54\,872$). Magnetization of the nanocube was determined by the quantum Monte-Carlo simulations[13] with Hamiltonian H,

$$H=\sum_{i,j} J_{ij}S_iS_j, \quad \text{where } J_{ij}=\begin{cases} J_o & (i,j\in \text{cube, n.n.}),\\ 0 & (\text{others}),\end{cases} \tag{2}$$

using Wolff algorithm.[14] At given temperatures, randomly selected spins on the limited lattice sites are flipped according to a probability related to the Boltzmann factor, until a stationary condition comes. The exchange interaction J_o was determined to reproduce the bulk Curie temperature at $N\rightarrow\infty$. At $L>20$ ($N>8{,}000$), the dependence is almost the same as the bulk Ni. At $L<20$ ($N<8000$), more rapid decrease of M_s than the bulk with increasing temperature and a residual magnetization above the bulk Curie temperature are observed. At $5<L<10$ ($N\sim 125-1000$), a good agreement is obtained between the simulation curves and the experimental results up to ~ 350 °C. Judging from the good agreements, possible origins of the characteristic behaviors observed in Ni NPs are speculated: The finiteness in the number of constituent atoms induces fluctuations of the moments to act against the ordering, resulting in more rapid decrease of M_s than the bulk with increasing temperature and a residual magnetization above the bulk Curie temperature. The existence of the NP surfaces as boundaries might also contribute to the instability of the magnetic ordering. The insufficient cancellation of randomly oriented spins due to the finite number of constituent atoms also contributes to the residual magnetization. However, as written before, the Langevin fitting gives $\sim 4\times 10^3$ spins per NP, while the simulation gives 125–1000 spins per NP. The agreements between experimental results and simulations are limited in a qualitative way.

In conclusion, we have studied temperature dependence of magnetization of Ni NPs in SiO_2 by the magneto-optical Kerr effects, in comparisons with the Ni thick film with the bulk nature. The saturation magnetization of Ni NPs decreases more steeply than the bulk Ni. However, a small but a nonzero value of magnetization remains in the NPs even above the bulk Curie temperature. From quantum Monte-Carlo simulation using a nanocube of the Ising fcc lattice, the experimental results of the Ni NPs are ascribed to the finite size effects of NPs.

A part of this study was financially supported by the Budget for Nuclear Research of the MEXT, based on the screening and counseling by the Atomic Energy Commission.

*Corresponding author; electronic address: amekura.hiroshi@nims.go.jp

[1] S. Sugano and H. Koizumi, *Microcluster Physics*, 2nd ed. (Springer-Verlag, Berlin, 1998).
[2] H. Haberland, *Clusters of Atoms and Molecules I & II* (Springer-Verlag, Berlin, 1994).
[3] M. Solzi, M. Ghidini, and G. Asti, in *Magnetic Nanostructures*, edited by H. S. Nalwa (American Sci., Los Angeles, 2002), Chap. 4.
[4] R. H. Kodama, J. Magn. Magn. Mater. **200**, 359 (1999).
[5] D. L. Leslie-Pelecky and R. D. Rieke, Chem. Mater. **8**, 1770 (1996).
[6] V. I. Nikolaev, T. A. Bushina, and K. E. Chan, J. Magn. Magn. Mater. **213**, 213 (2000).
[7] N. Kishimoto, Y. Takeda, V. T. Gritsyna, E. Iwamoto, and T. Saito, in *IEEE Transactions from 1998 International Conference on Ion Implantation Technology Proceedings*, edited by J. Matsuo, G. Takaoka, and I. Yamada (IEEE, Piscataway, 1999), p. 342.
[8] J. F. Ziegler, J. P. Biersack, and U. Littmark, *The Stopping and Range of Ions in Solids* (Pergamon, New York, 1985), Chap. 8; available from http://www.srimg.org/.
[9] H. Amekura, H. Kitazawa, N. Umeda, Y. Takeda, and N. Kishimoto, Nucl. Instrum. Methods Phys. Res. B **222**, 114 (2004).
[10] H. Amekura, Y. Takeda, K. Kono, and N. Kishimoto, Trans. Mater. Res. Soc. Jpn. **29**, 623 (2004).
[11] C. Kittel, *Introduction to Solid State Physics*, 7th ed. (Wiley & Sons, New York, 1996), Chap. 15, p. 448.
[12] H. Amekura, H. Kitazawa, and N. Kishimoto, Nucl. Instrum. Methods Phys. Res. B **219–220**, 825 (2004).
[13] J. J. Binney, N. J. Dowrick, A. J. Fisher, and M. E. J. Newman, *The Theory of Critical Phenomena: An Introduction to the Renormalization Group* (Oxford University Press, Oxford, 1992), Chap. 4.
[14] U. Wolff, Phys. Rev. Lett. **62**, 361 (1989).